

Supplementary Information

This file includes:

Supplementary Figure Legends

Supplementary Figures 1-7

Supplementary Tables 1-3

SUPPLEMENTARY FIGURE LEGENDS

Supplementary Figure 1. Antisense transcription in the human C-MYC locus. (A)

Antisense reads in polyA-depleted (top), polyA-enriched (middle) nuclear RNA and polyA-enriched cytosolic RNA (bottom) in the c-MYC 3' distal region in K562 cells detected by RNA-Seq. (B) Levels of c-MYC mRNA and antisense transcripts in human prostate cancer cell lines determined by RT-PCR and strand-specific RT-PCR, respectively.

Supplementary Figure 2. RNA Polymerase 2 (RNAPol2) occupancy within the c-MYC

locus. RNAPol2 binding was determined by chromatin immunoprecipitation in PC3 cells incubated with vehicle (DMSO) or SAHA (2.5-10 µM) for 6 h. Data are presented as fold enrichment relative to input DNA.

Supplementary Figure 3. 5' extension of antisense transcripts in the c-MYC 3' UTR.

5'RACE was performed with the indicated primers starting from position +4772 in the c-MYC exon 3.

Supplementary Figure 4. c-MYC mRNA and antisense transcripts in immortalized

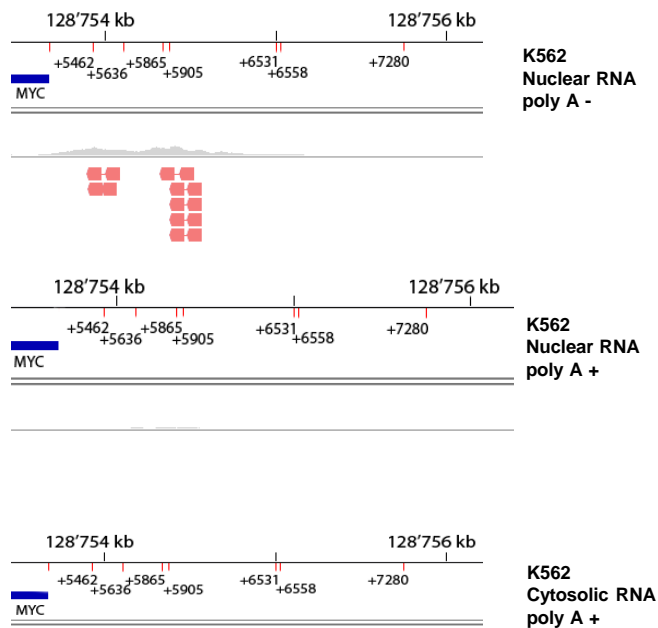
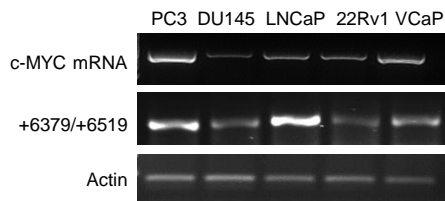
normal prostate epithelial cells. Cells were incubated in culture medium (control) or treated with vehicle (DMSO) or SAHA (2.5-10 µM).

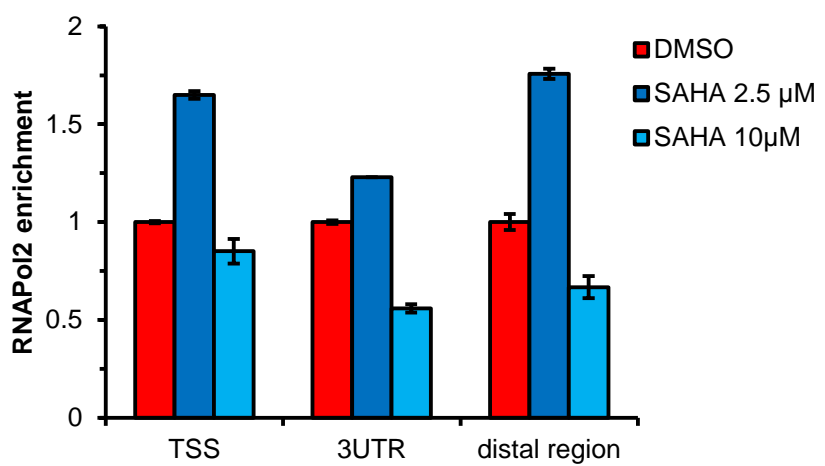
Supplementary Figure 5. Putative binding sequence of NAT6531-derived sRNA5 in the

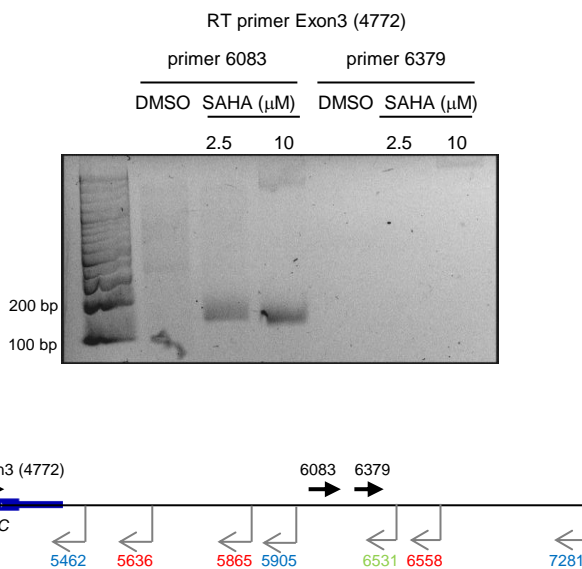
c-MYC locus. Matching miRNA-like binding sites for sRNA5 (top panel) were predicted searching within the c-MYC locus using StarMiR. Four sites (three in the promoter region and one in intron 1) of the top sites with best fit to canonical miRNA binding mode are shown.

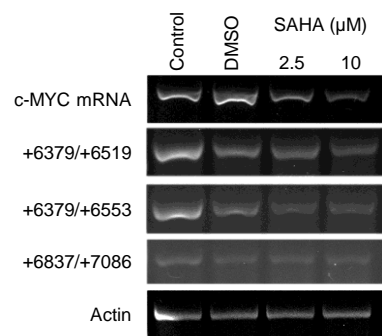
Supplementary Figure 6. Dicer knockdown efficiency and production of endogenous small RNA in PC3 cells. (A) Level of Dicer mRNA in PC3 cells transfected with siGL3 or siDicer. (B) Northern blot analysis of long and small RNAs in PC3 cells after depletion of Dicer for 72 h and treatment with SAHA for 6 h. Left and right panels show a longer and shorter exposure, respectively, of the same blot after hybridization with RNA probe 5866-6558. *In vitro* transcribed (IVT) NAT6531 or NAT6558 after Dicer digestion were loaded in parallel as reference along with Dicer digested NAT6531 after fractionation in short (<200 nt) and long (>200 nt) RNA. Gray and black arrows indicate the position of long NATs and small RNAs, respectively. (C) Position of RNA probe 5865-6558 respect to antisense transcripts.

Supplementary Figure 7. c-MYC mRNA levels in Dicer depleted PC3 cells. c-MYC mRNA and antisense transcripts in PC3 cells incubated with control (siGL3) and Dicer targeting (siDicer) siRNA were determined by RT-PCR and strand-specific RT-PCR, respectively.

A**B**







Supplementary Figure 5

sRNA5 (miRNA) 5'-AGUGAAUCUUGGGCAUG-3'

PROMOTER

Site 6

Site 9

5'→3'		A	AUC	G	
Target	219	GUGC	GGAUUUG		232
miRNA	17	UACG	UCUAAGU		1
3'→5'		G	GGU	GA	

Site 10

5'→3'		A	ACUAU	U	
Target	236	GCU	AUUCACU		250
miRNA	17	CGG	UAAGUGA		1
3'→5'		GUA	GUUC		

Site 17

5'→3'		U	AAUA	C	G	
Target	567	GUG	CA	GUUUGC		582
miRNA	17	UAC	GU	UAAGUG		1
3'→5'		G	GG	UC	A	

Site 23

5' ->3'		C		U
Target	818	GUCC	GGUUUG	827
miRNA	17	CGGG	CUAAGU	1
3' ->5'		GUA	UU	GA

Site 43

The diagram illustrates the binding site of a miRNA on its target mRNA. The target sequence is 5'→3' (top) and 3'→5' (bottom). The miRNA sequence is 3'→5' (top) and 5'→3' (bottom). The binding region is highlighted in green, showing conservation between species. The mature miRNA (red) and precursor hairpin (blue) are also indicated.

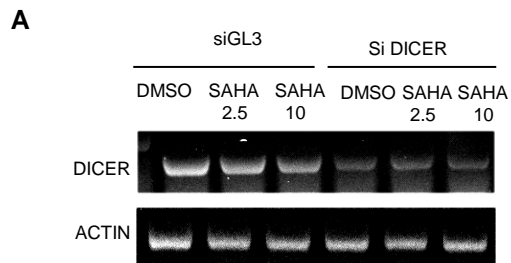
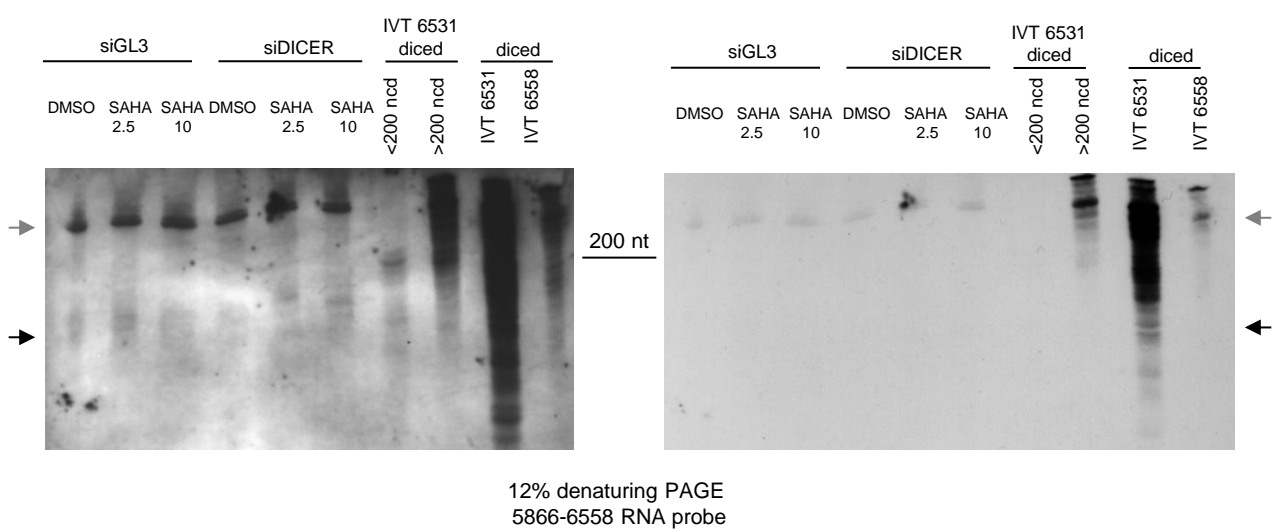
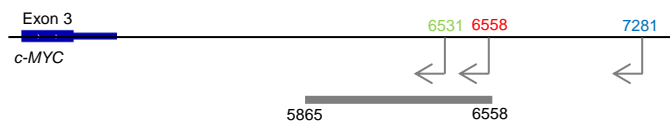
INTRON 1

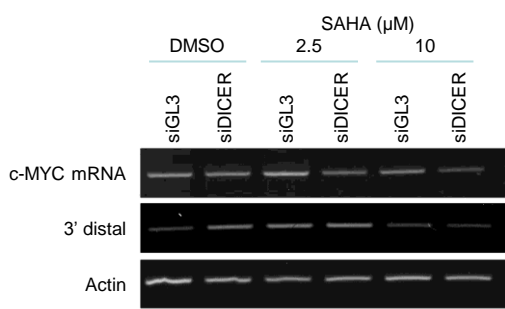
Site 6

5' ->3'
Target 2575 U UUUUA U
 UGCCU AUUUUAU 2590
miRNA 17 ACGGG UAAGUGA 1
3' ->5'
 GU UUC

Site 70

5'→3'		C	UAUGAAUAU	G	
Target	2811	UGCCU	AUUCAC		2830
miRNA	17	ACGGG	UAAGUG		1
3'→5'		GU	UUC	A	

**B****C**



Supplementary Table 1 - Primer sets

Primer name	Primer sequence	Application
Myc exon1 +100 Fw	ggagatccggaggcgaatag	RT-PCR
Myc intron1+463 Rev	gcattcgactcatctcagca	RT-PCR
MYC exon2 +2202 Rev	cagctcgaaattcttccagata	RT-PCR
MYC exon 3 +4772 Fw	tgtcctgagcaatcacatcg	RT-PCR, RACE
MYC 3'UTR +5374 Fw	aagatgcttcctggagactatga	RT-PCR, RACE
MYC 3'UTR +5526 Rev	cccaactccccagtcccttat	RT-PCR
Myc +5430 Fw	aggcaggtgagaagggtgaga	RACE
Myc +6083 Fw	ggggaaaagtggaaagcgagat	RACE
Myc+6130 Fw	ctgtccaagccacacctca	RACE
Myc +6379 Fw	ctgggaagaagccagttcag	RT-PCR, RACE
Myc +6519 Rev	tcaaggactcaggatgagca	RT-PCR
T7 prom +as 6531 rev	gcgttaatcgcactcaactatagggagaaaaaacatcttcaaggac	IVT
T7 prom +as 6558 rev	gcgttaatcgcactcaactatagggagataggttcagaggcttat	IVT
T7 prom +myc 5866 Fw	gcgttaatcgcactcaactatagggagagtctaattgtgctgagatcaaga	IVT
T7 prom +myc 5906 Fw	gcgttaatcgcactcaactatagggagaacacagactcaagtcataacaatg	IVT
T7 prom +myc 6060 Fw	gcgttaatcgcactcaactatagggagacacatgccaaaggattcactgat	IVT
T7 prom +myc 5930 Fw1	gcgttaatcgcactcaactatagggagaaaggcttatttgtgtccaaagc	IVT
T7 prom +myc 6086 Fw	gcgttaatcgcactcaactatagggagagaaaagtggaaagcgagatttg	IVT
myc +6113 rev	ctgggtcaaactcgcttc	IVT
myc +6256 Rev	ggggaaactgtgcctgac	IVT
As 5866 Fw	gtctaatgtgctgagatcaaga	IVT, RT-PCR
As 5906 Fw	acagactcaagtcataacaatg	IVT, RT-PCR
As 6060 Fw	cacatgccaaaggattcactgat	RT-PCR
As 6531 Rev	aaaaaacatcttcaaggac	RT-PCR
As 6558 Rev	tagtttcagaggcttat	RT-PCR
Myc exon2 qPCR Fw	ggtgctccatgaggagaca	qRT PCR
Myc exon 3 qPCR Rev	cctgcctttccacagaa	qRT PCR
ACTB+832 Fw 1	attggcaatgagcggttc	qRT PCR
ACTB +907 Rev 1	ggatgccacaggactccat	qRT PCR

Supplementary Table 2 - GRO-Seq data sets

Cell line	Dataset series	Reference
AC16	GSE41323	Danko CG, Hah N, Luo X, Martins AL et al. Signaling pathways differentially affect RNA polymerase II initiation, pausing, and elongation rate in cells. <i>Mol Cell</i> 2013 Apr 25;50(2):212-22. PMID: 23523369
Hela_danko	GSE62046	Andersson R, Refsing Andersen P, Valen E, Core LJ et al. Nuclear stability and transcriptional directionality separate functionally distinct RNA species. <i>Nat Commun</i> 2014 Nov 12;5:5336. PMID: 25387874
Hela_laitem	E-MTAB-3360	Laitem C, Zaborowska J, Isa NF, Kuks J, Dienstbier M, Murphy S. CDK9 inhibitors define elongation checkpoints at both ends of RNA polymerase II-transcribed genes. <i>Nat Struct Mol Biol</i> . 2015 May;22(5):396-403. doi: 10.1038/nsmb.3000. Epub 2015 Apr 6. PMID:25849141
Hela_duttke	GSE63872	Duttke SH, Lacadie SA, Ibrahim MM, Glass CK et al. Human promoters are intrinsically directional. <i>Mol Cell</i> 2015 Feb 19;57(4):674-84. PMID: 25639469
IMR90	GSE13518	Core LJ, Waterfall JJ, Lis JT. Nascent RNA sequencing reveals widespread pausing and divergent initiation at human promoters. <i>Science</i> 2008 Dec 19;322(5909):1845-8. PMID: 19056941
LNCaP	GSE 47807	Yang et al. Yang L, Lin C, Jin C, Yang JC, Tanasa B, Li W, Merkurev D, Ohgi KA, Meng D, Zhang J, Evans CP, Rosenfeld MG. <i>Nature</i> . 2013 Aug 29;500(7464):598-602.doi:10.1038/nature12451.Epub 2013 Aug 14.PMID: 23945587
LNCaP	GSE27823	Wang D, Garcia-Bassets I, Benner C, Li W et al. Reprogramming transcription by distinct classes of enhancers functionally defined by eRNA. <i>Nature</i> 2011 May 15;474(7351):390-4. PMID: 21572438
K562	GSE66448	Niskanen EA, Malinen M, Sutinen P, Toropainen S et al. Global SUMOylation on active chromatin is an acute heat stress response restricting transcription. <i>Genome Biol</i> 2015 Jul 28;16:153. PMID: 26259101
BT474, MCF10, SKBR3, ZR75-30	E-MTAB-666, E-MTAB-667, E-MTAB-668 and E-MTAB-675	Kim YJ, Greer CB, Cecchini KR, Harris LN, Tuck DP, Kim TH. HDAC inhibitors induce transcriptional repression of high copy number genes in breast cancer through elongation blockade. <i>Oncogene</i> . 2013 Jun 6;32(23):2828-35. doi: 10.1038/onc.2013.32. Epub 2013 Feb 25.PMID:23435418
GM12004, GM12750	GSE39878	Wang IX, Core LJ, Kwak H, Brady L et al. RNA-DNA differences are generated in human cells within seconds after RNA exits polymerase II. <i>Cell Rep</i> 2014 Mar 13;6(5):906-15. PMID: 24561252
h1ESC	GSE41009	Sigova AA, Mullen AC, Molinie B, Gupta S et al. Divergent transcription of long noncoding RNA/mRNA gene pairs in embryonic stem cells. <i>Proc Natl Acad Sci U S A</i> 2013 Feb 19;110(8):2876-81. PMID: 23382218
HCT116 p53 +/+, p53 -/-	GSE53964	Allen MA, Andrysiak Z, Dengler VL, Mellert HS et al. Global analysis of p53-regulated transcription identifies its direct targets and unexpected regulatory mechanisms. <i>Elife</i> 2014 May 27;3:e02200. PMID: 24867637
MCF7	GSE45822	Li W, Notani D, Ma Q, Tanasa B et al. Functional roles of enhancer RNAs for oestrogen-dependent transcriptional activation. <i>Nature</i> 2013 Jun 27;498(7455):516-20. PMID: 23728302

Supplementary table 3 - StarMiR predicted binding sites of sRNA5 in the C-MYC locus

PROMOTER-5'UTR								
Site ID	Site_Position	LogitProb	3'_bp	ΔGhybrid	ΔGnuc	ΔGtotal	Site_Access	Site_Location
1	5-16	0.527	0	-16.7	-0.9	-4.203	0.367	0.003
2	39-54	0.48	1	-18.6	-0.123	0.955	0.302	0.02
3	90-96	0.487	1	-16.4	-0.068	-0.081	0.168	0.045
4	90-99	0.519	1	-17.6	-0.064	4.32	0.12	0.045
5	90-105	0.619	1	-18.1	-0.064	13.891	0.081	0.045
6	150-165	0.444	0	-14	-1.035	8.398	0.305	0.075
7	173-195	0.491	0	-13.8	-0.169	8.54	0.292	0.087
8	219-238	0.427	0	-15.8	-0.9	-6.438	0.503	0.11
9	219-232	0.449	0	-14.8	-0.878	-5.091	0.406	0.11
10	236-250	0.238	0	-15.3	-0.97	-11.343	0.606	0.118
11	309-324	0.453	1	-15.2	-5.214	-4.102	0.598	0.155
12	357-382	0.402	0	-13.5	-0.088	9.501	0.335	0.179
13	387-398	0.588	1	-16.3	-0.005	-0.755	0.188	0.194
14	435-445	0.573	1	-18.3	-0.671	-7.051	0.335	0.218
15	435-452	0.542	1	-20.1	-0.671	-6.323	0.403	0.218
16	463-479	0.431	0	-15.3	-1.716	-7.364	0.437	0.232
17	567-582	0.523	0	-10.4	-0.207	-3.283	0.402	0.284
18	595-607	0.608	0	-16.3	-0.561	-4.918	0.305	0.298
19	649-660	0.581	1	-15.5	-0.386	-6.773	0.438	0.325
20	649-664	0.564	1	-15.8	-0.386	-4.161	0.415	0.325
21	678-688	0.613	0	-17.9	-0.956	-9.018	0.362	0.339
22	678-685	0.596	0	-17.2	-0.956	-8.83	0.414	0.339
23	818-827	0.569	0	-12.1	-3.979	-7.765	0.465	0.409
24	826-834	0.715	0	-16.8	-0.029	-3.104	0.159	0.413
25	907-920	0.477	1	-15.1	-0.005	9.601	0.075	0.454
26	907-925	0.419	1	-15.3	-0.005	12.144	0.111	0.454
27	924-939	0.452	0	-17.1	-0.014	5.92	0.2	0.462
28	1002-1009	0.669	0	-19.9	-6.141	-12.928	0.608	0.501
29	1002-1016	0.604	0	-21.9	-6.256	-12.146	0.481	0.501
30	1002-1013	0.62	0	-19.9	-6.141	-11.534	0.551	0.501
31	1020-1048	0.499	0	-13.8	-2.564	4.379	0.491	0.51
32	1020-1051	0.486	0	-13.9	-2.564	7.201	0.467	0.51
33	1025-1033	0.608	0	-15.3	-0.274	-5.849	0.445	0.513
34	1025-1036	0.612	0	-17.6	-0.312	-4.193	0.348	0.513
35	1150-1163	0.44	0	-15.8	0	9.127	0.188	0.575
36	1156-1180	0.494	0	-16.6	-0.643	-0.486	0.422	0.578
37	1358-1375	0.598	1	-12.9	-0.699	8.122	0.179	0.679
38	1358-1378	0.577	1	-14	-0.696	10.265	0.155	0.679
39	1452-1466	0.63	1	-15.5	-1.778	-2.436	0.521	0.726
40	1573-1587	0.397	0	-15.6	-0.026	-0.954	0.231	0.787
41	1586-1604	0.261	0	-16.7	-0.01	11.65	0.196	0.793
42	1660-1681	0.708	0	-17.7	-0.022	-9.387	0.553	0.83
43	1660-1675	0.758	0	-16.9	-4.268	-8.588	0.59	0.83
44	1691-1700	0.76	1	-9.7	-0.008	0.952	0.208	0.846
45	1741-1748	0.613	0	-9.6	-0.024	5.203	0.199	0.871
46	1775-1791	0.64	0	-13.5	-3.837	3.753	0.503	0.888
47	1795-1813	0.614	0	-12.9	-2.871	-2.588	0.536	0.898
48	1837-1843	0.662	1	-15.3	-4.612	-8.891	0.466	0.919
49	1837-1850	0.494	1	-16.2	-4.612	-1.809	0.306	0.919
50	1837-1847	0.525	1	-15.4	-4.612	-1.282	0.359	0.919
51	1892-1908	0.688	0	-17.9	-2.865	-6.604	0.455	0.946
52	1892-1906	0.619	0	-16.4	-2.865	-4.015	0.485	0.946
53	1960-1976	0.629	0	-16	-3.142	-0.981	0.499	0.98

CODING SEQUENCE-CDS								
Site ID	Site_Position	LogitProb	3'_bp	ΔGhybrid	ΔGnuc	ΔGtotal	Site_Access	Site_Location
54	2002-2017	0.133	0	-16.7	-0.006	-7.466	0.639	0.001
55	2039-2053	0.056	0	-15.8	-0.04	13.035	0.067	0.007
56	2065-2074	0.16	1	-17.2	0	-4.372	0.523	0.012
57	2301-2316	0.167	0	-17.3	-0.023	7.703	0.195	0.056
58	2326-2338	0.292	0	-15.3	0	-4.295	0.381	0.061
59	2364-2369	0.676	1	-15.8	-1.781	-12.639	0.556	0.068
60	2364-2376	0.459	1	-16.9	-1.781	-9.445	0.486	0.068
61	2364-2373	0.532	1	-16.3	-1.781	-9.439	0.538	0.068
62	2364-2387	0.545	1	-19	-1.826	-0.641	0.412	0.068
63	2472-2491	0.449	0	-16.2	-0.426	-5.363	0.623	0.088
64	2544-2563	0.543	0	-15.1	-0.025	-2.531	0.482	0.102
65	2560-2574	0.793	0	-15.9	-2.088	-8.784	0.567	0.105
66	2575-2590	0.838	1	-14.9	-4.32	-9.637	0.71	0.107
67	2622-2629	0.669	1	-15.8	-0.013	-11.626	0.609	0.116
68	2622-2636	0.461	1	-16.4	0	-0.086	0.523	0.116
69	2622-2640	0.498	1	-16.7	0	0.73	0.42	0.116
70	2811-2830	0.438	1	-17	-4.615	-11.343	0.606	0.151
71	2875-2888	0.388	0	-15.8	-0.476	1.321	0.258	0.163
72	2875-2897	0.327	0	-16.4	-0.476	10.041	0.27	0.163
73	2966-2986	0.408	0	-16.1	-5.512	0.603	0.385	0.18